

γ/ϕ_3 @ ee colliders



**Yoshiyuki Onuki
Tohoku University
On behalf of Belle**

On Earthquake

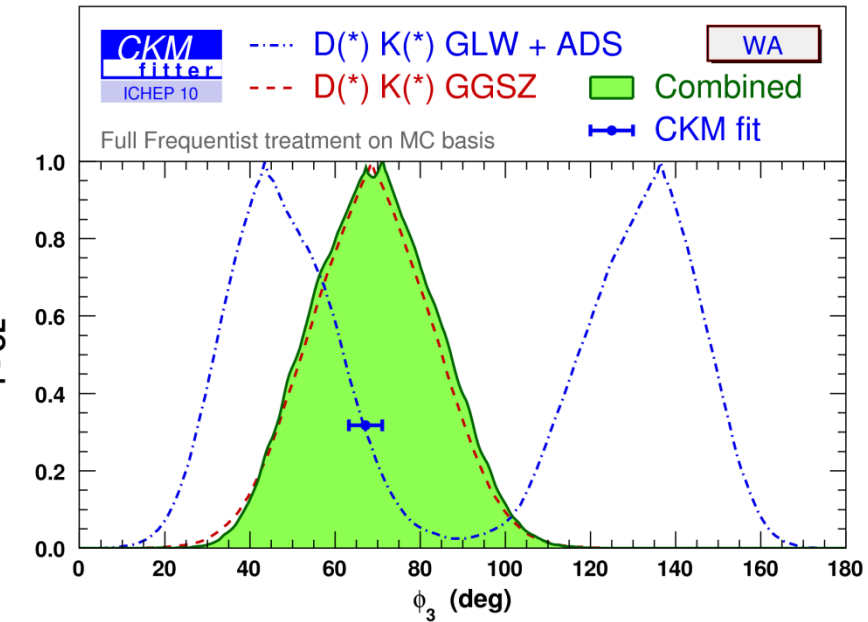
As is now well known, Japan suffered a terrible earthquake and tsunami on March 11, which has caused tremendous damage, especially in the Tohoku area.

Fortunately, all KEK personnel and users are safe and accounted for. The injection linac did suffer significant but manageable damage, and repairs are underway. The damage to the KEKB main rings appears to be less serious, though non-negligible. No serious damage has been reported so far at Belle. Further investigation is necessary.

We would like to convey our deep appreciation to everyone for your generous expressions of concern and encouragement.

Outline

- Introduction
- γ/ϕ_3 measurements
- Experimental apparatus
- GGSZ results
- ADS results
- GLW results
- Summary



Introduction

N. Cabibbo, PRL.10, 531 (1963); M. Kobayashi and T. Maskawa, Prog. Theor. Phys. 49, 652 (1973).
 I. I. Bigi and A. I. Sanda, Phys. Lett. B 211, 213 (1988).

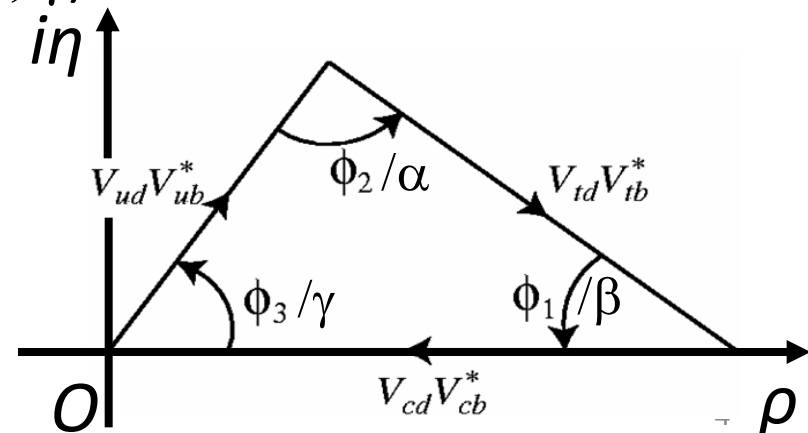
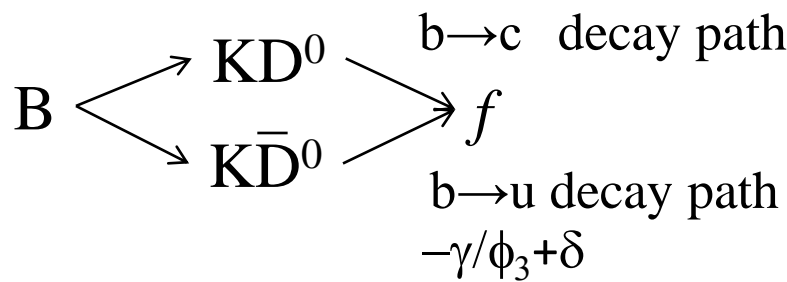
In the Standard Model, irreducible complex phase in Cabibbo-Kobayashi-Maskawa (CKM) matrix cause the CP violation.

$$V_{n=3} = \begin{pmatrix} V_{ud} & V_{us} & V_{ub} \\ V_{cd} & V_{cs} & V_{cb} \\ V_{td} & V_{ts} & V_{tb} \end{pmatrix} \simeq \begin{pmatrix} 1 - \lambda^2/2 & \lambda & A\lambda^3(\rho - i\eta) \\ -\lambda & 1 - \lambda^2/2 & A\lambda^2 \\ A\lambda^3(1 - \rho - i\eta) & -A\lambda^2 & 1 \end{pmatrix}$$

One of the unitarity condition of CKM:

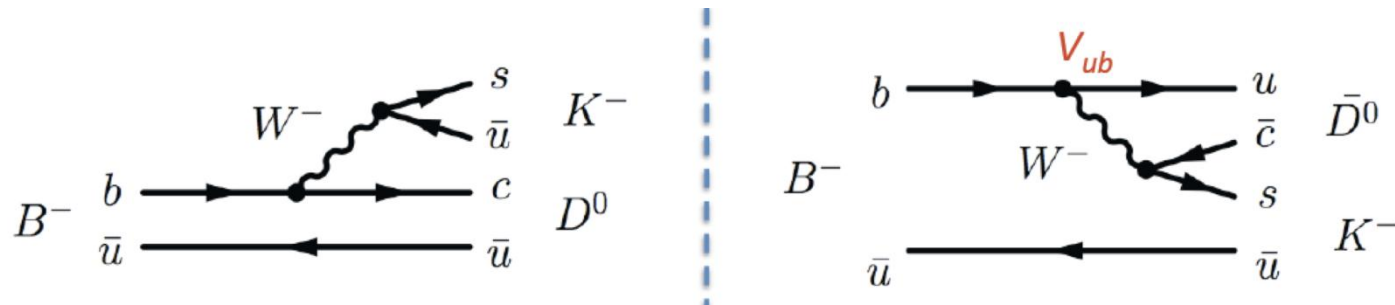
$$V_{ud}V_{ub}^* + V_{cd}V_{cb}^* + V_{td}V_{tb}^* = 0$$

$$(\phi_1, \phi_2, \phi_3) = (\beta, \alpha, \gamma)$$



γ/ϕ_3 measurements

Interference between tree diagram $b \rightarrow c$ and $b \rightarrow u$ ($V_{ub} \propto e^{-i\phi_3}$)
in charged $B \rightarrow D^{(*)0} K^{(*)}$ or self-tagging neutral $B^0 \rightarrow D^{(*)0} K^{*0}$ ($K^{*0} \rightarrow K^+ \pi^-$)



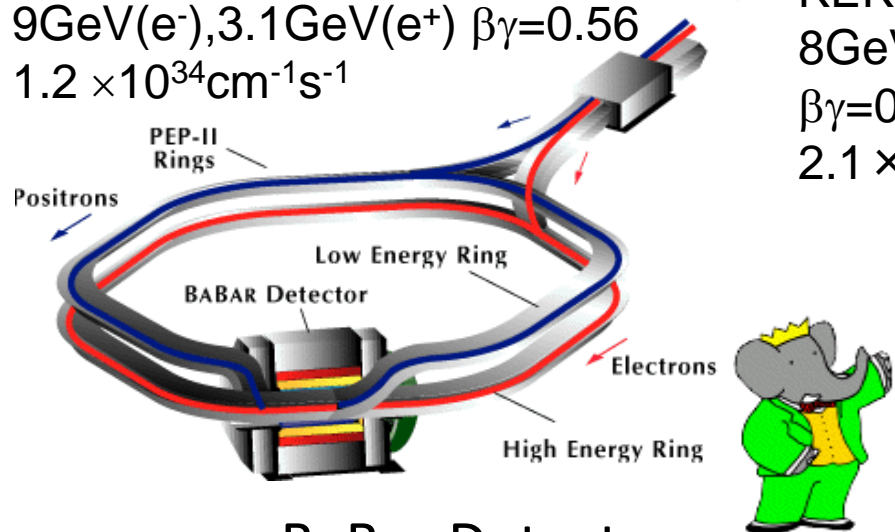
- GGSZ: Cabibbo favored multibody decays with Dalitz plane
- ADS: doubly Cabibbo suppressed
- GLW: CP eigenstates (Cabibbo suppressed)

ee collider B-factories

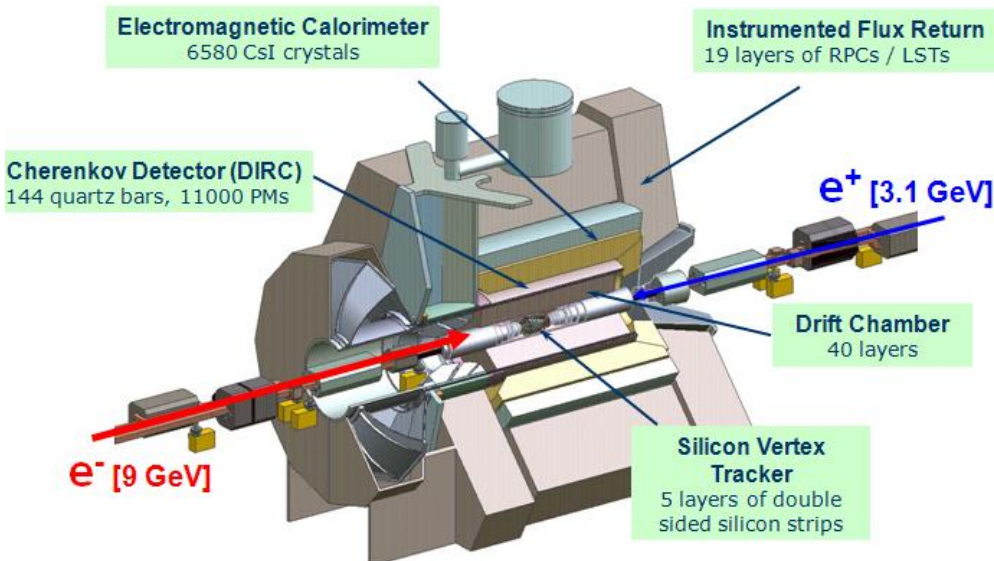
PEP-II

$9\text{GeV}(e^-), 3.1\text{GeV}(e^+)$ $\beta\gamma=0.56$

$1.2 \times 10^{34}\text{cm}^{-1}\text{s}^{-1}$



BaBar Detector

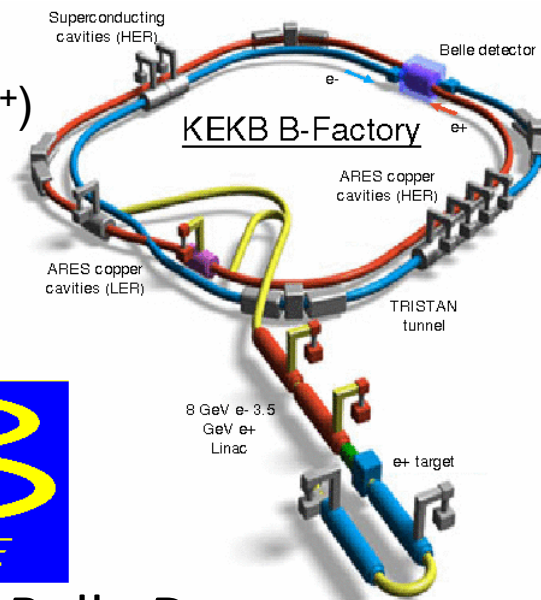


KEKB

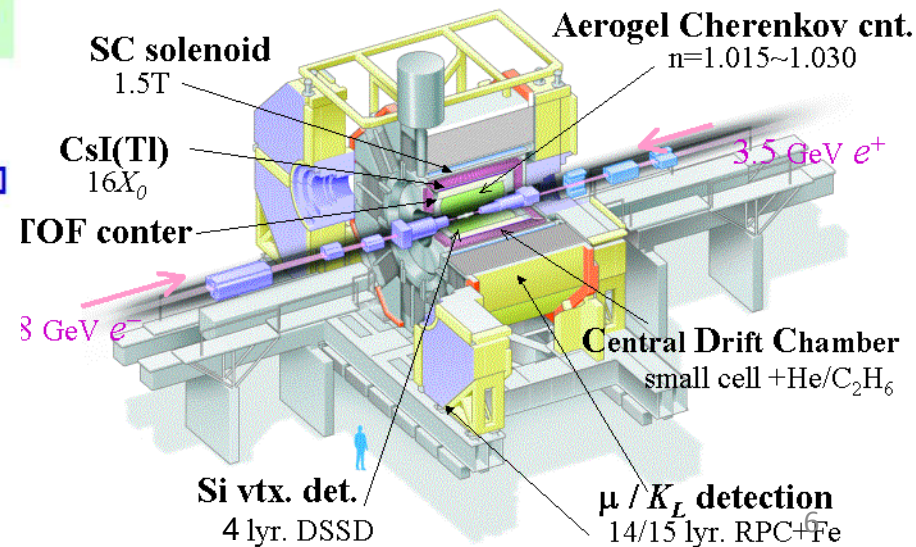
$8\text{GeV}(e^-) \times 3.5\text{GeV}(e^+)$

$\beta\gamma=0.425$

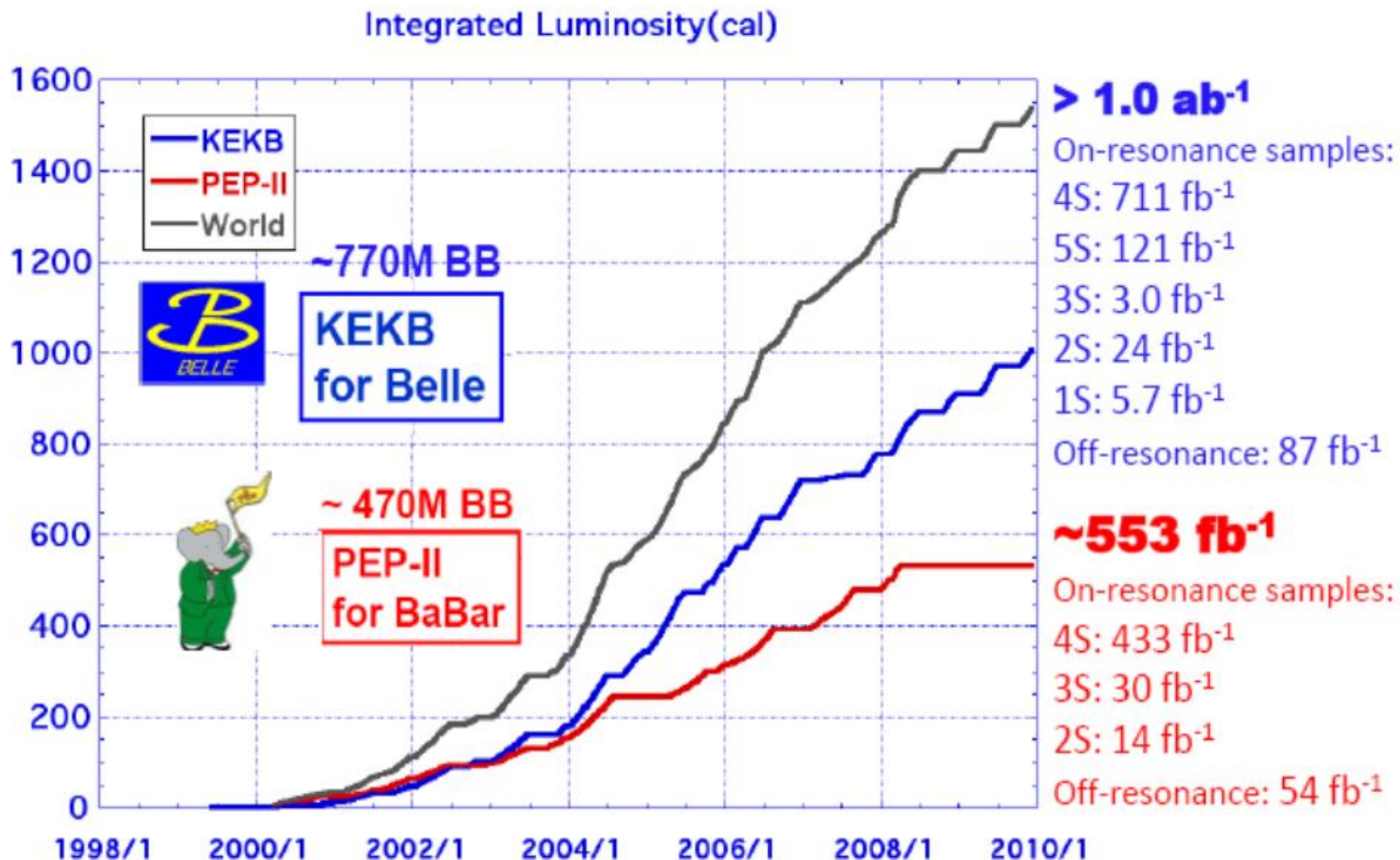
$2.1 \times 10^{34}\text{cm}^{-2}\text{s}^{-1}$



Belle Detector



Integrated Luminosity at B-factories



Dalitz Plot(DP) Analysis of $B^- \rightarrow D^{(*)} K^{(*)-}$ $D \rightarrow K_S h^+ h^-$

A. Bondar, Belle Dalitz analysis meeting, 24-26 Sep. 2002

A. Giri, Yu. Grossman, A. Soffer, J. Zupan, PRD 68, 054018 (2003)

Application of $B^\pm \rightarrow DK^\pm$

Using D meson decay into CP eigenstate 3-body $D \rightarrow K_S h^+ h^-$

$$m_+ \equiv M_{K_S h^+}, \quad m_- \equiv M_{K_S h^-}$$

Dalitz plot amp. $M_\pm(m_+, m_-)$:

$$M_\pm(m_+^2, m_-^2) = f(m_+^2, m_-^2) + r_B e^{\pm i\phi_3 + i\delta_B} f(m_-^2, m_+^2)$$

$$= \begin{array}{c} \text{[Diagram of a Dalitz plot showing a peak in the lower-right quadrant]} \\ + r_B e^{\pm i\phi_3 + i\delta_B} \begin{array}{c} \text{[Diagram of a Dalitz plot showing a peak in the upper-left quadrant]} \end{array} \end{array}$$

$f(m_+^2, m_-^2)$...consists of summing over the intermediate resonance amplitudes of $K_S h^+$ ($K_S h^-$) at each fraction.

r_B ...is ratio of interfering amplitudes of $A(B \rightarrow DK)$ and $A(B \rightarrow \bar{D}K)$
 $\sim |V_{ub}^* V_{cs}| / |V_{cb}^* V_{us}| \times \text{color suppression} \sim 0.1-0.2$

Model-dependent DP analysis

657M



A.Poluektov *et al.*,
PRD 81,112002(2010)

Belle: $D \rightarrow K_S \pi\pi$ produced in the $B^- \rightarrow D^{(*)} K^-$ where $D^* \rightarrow D\pi^0$ and $D\gamma$

468M



P. del Amo Sanchez *et al.*
PRL 105, 121801(2010)

BaBar: $D \rightarrow K_S \pi\pi$ and $D \rightarrow K_S KK$ produced in the $B^- \rightarrow D^{(*)} K^-$ and $B^- \rightarrow DK^{(*)-}$ where $D^* \rightarrow D\pi^0$ and $D\gamma$, $K^* \rightarrow K_S \pi$

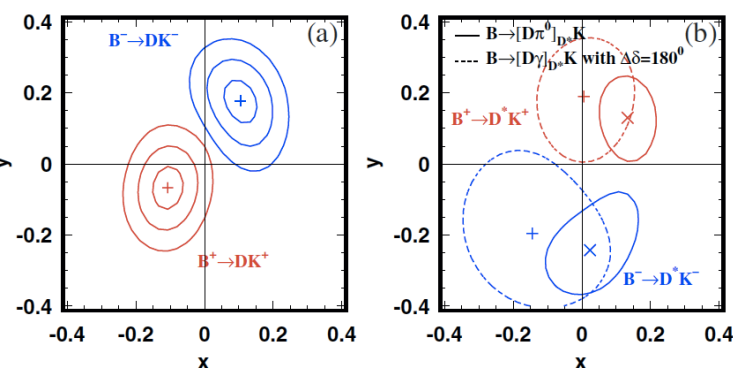
Unbinned model-dependent DP analysis with isobar model

| | | | | | |
|------------------------------|-----------|-----------------|------------------------------|-----------|----------------------------|
| $D^0 \rightarrow K_S \pi\pi$ | $\pi\pi$ | σ_1^0 | $D^0 \rightarrow K_S \pi\pi$ | $\pi\pi$ | $\omega(782)^0$ |
| | $\pi\pi$ | $\rho(770)^0$ | | $\pi\pi$ | $\rho(770)^0$ |
| | $\pi\pi$ | $\omega(782)^0$ | | $K_S \pi$ | $K^*(892)$ |
| | $\pi\pi$ | $f_0(980)^0$ | | $K_S \pi$ | $K^*(1680)^-$ |
| | $\pi\pi$ | σ_2^0 | | $\pi\pi$ | $f_2(1270)^0$ |
| | $\pi\pi$ | $f_2(1270)^0$ | | $K_S \pi$ | $K_0^*(1430), K_2^*(1430)$ |
| | $\pi\pi$ | $f_0(1370)^0$ | | $\pi\pi$ | S-wave K-matrix |
| | $\pi\pi$ | $\rho(1450)^0$ | | $K_S \pi$ | S-wave K-matrix |
| | $K_S \pi$ | $K^*(892)$ | | KK_S | $a_0(980)$ |
| | $K_S \pi$ | $K^*(1410)$ | | KK_S | $a_0(1450)$ |
| | $K_S \pi$ | $K_2^*(1430)$ | | KK | $a_0(980)^0$ |
| | $K_S \pi$ | $K^*(1680)$ | | KK | $a_0(1450)^0$ |
| $D^0 \rightarrow K_S KK$ | | | | KK | $f_0(1370)^0$ |
| $D^0 \rightarrow K_S KK$ | | | | KK | $\phi(1020)^0$ |
| $D^0 \rightarrow K_S KK$ | | | | KK | $f_2(1270)^0$ |

Model-dependent DP analysis results

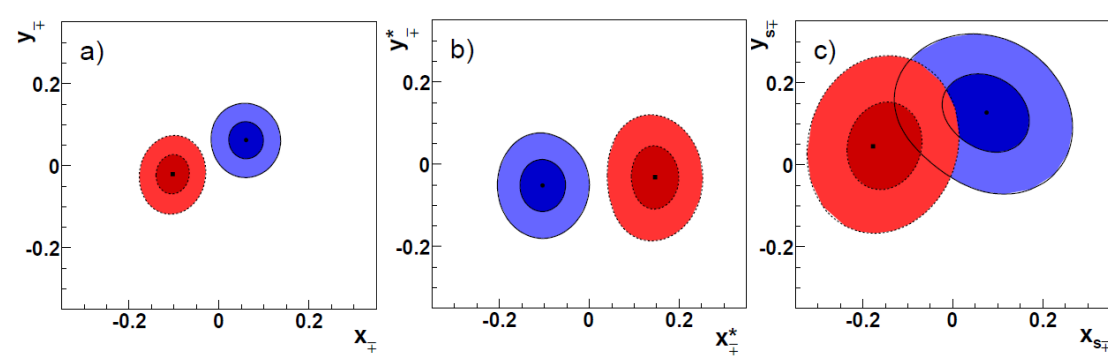


A.Poluektov *et al.*,
PRD 81,112002(2010)



468M

P. del Amo Sanchez *et al.*,
PRL 105, 121801(2010)



Combining the results for $B \rightarrow D^{(*)} K$

$$\phi_3 = (78.4^{+10.8}_{-11.6} \pm 3.6 \pm 8.9(\text{model}))^\circ$$

$$r_{DK} = 0.160^{+0.040}_{-0.038} \pm 0.011^{+0.050}_{-0.010}$$

$$r_{D^* K} = 0.196^{+0.072}_{-0.069} \pm 0.012^{+0.062}_{-0.012}$$

$$\delta_{DK} = 136.7^\circ {}^{+13.0^\circ}_{-15.8^\circ} \pm 4.0^\circ \pm 22.9^\circ$$

$$\delta_{D^* K} = 341.9^\circ {}^{+18.0^\circ}_{-19.6^\circ} \pm 3.0^\circ \pm 22.9^\circ$$

Combining the results for $B \rightarrow D^{(*)} K^{(*)}$

$$\phi_3 = (68 \pm 14 \pm 4 \pm 3(\text{model}))^\circ$$

$$r_B = 9.6 \pm 2.9 \{0.5, 0.4\}$$

$$r^* B = 13.3^{+4.2}_{-3.9} \{1.3, 0.3\}$$

$$\kappa r_s = 14.9^{+6.6}_{-6.2} \{2.6, 0.6\}$$

$$\delta_B = 119^{+19}_{-20} \{3, 3\}$$

$$\delta_B^* = -82 \pm 21 \{5, 3\}$$

$$\delta_s = 111 \pm 32 \{11, 3\}$$

Where { , } is
{experimental, model}
systematic uncertainties.

Model-independent binned DP analysis

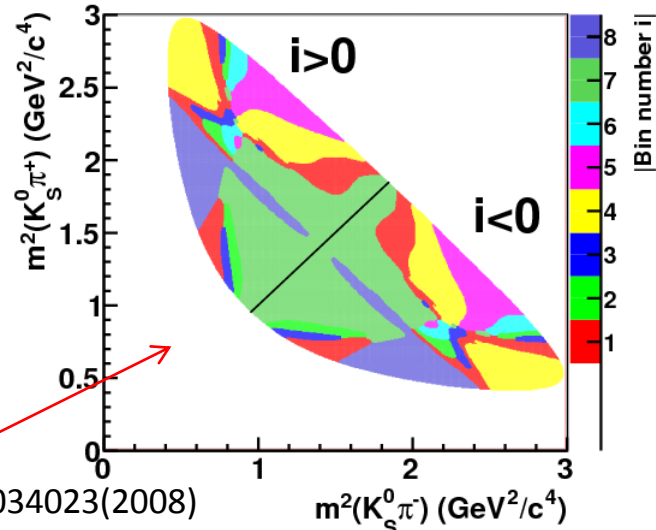
new
772M
Belle Preliminary



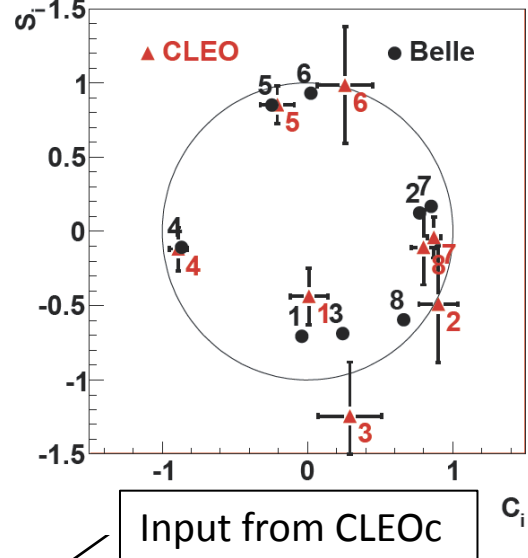
Model-independent optimal binned DP analysis

A. Giri, Yu. Grossman, A. Soer, J. Zupan, PRD 68, 054018 (2003)
 A. Bondar, A. Poluektov, EPJ C 47, 347 (2006); EPJ C 55, 51 (2008)

Binning is chosen to minimize the strong phase difference $\Delta\delta_D$ between $D^0 \rightarrow K_S \pi\pi$ and $\bar{D}^0 \rightarrow K_S \pi\pi$ from the isobar model.



Isobar model(PR D 78, 034023(2008)
 previous meas. by BaBar) is used
 for only binning



$$M_i^\pm = h \{ K_i + r_B^2 K_{-i} + 2 \sqrt{K_i K_{-i}} (x_\pm c_i + y_\pm s_i) \}$$

where $\begin{cases} M_i^\pm: \text{numbers of events in } D \rightarrow K_S^0 \pi^+ \pi^- \text{ bins from } B^\pm \rightarrow D K^\pm \\ x_\pm = r_B \cos(\delta_B \pm \phi_3) \quad y_\pm = r_B \sin(\delta_B \pm \phi_3) \\ c_i = \langle \cos \Delta \delta_D \rangle, s_i = \langle \sin \Delta \delta_D \rangle \end{cases}$

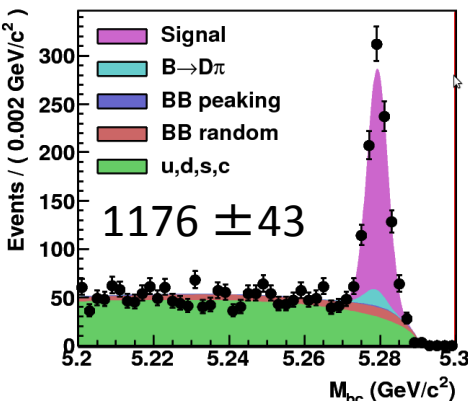
K_i : numbers of events in bins of flavor $\bar{D}^0 \rightarrow K_S^0 \pi^+ \pi^-$ from $D^* \rightarrow D \pi$.

Model-independent Binned DP yield and plot

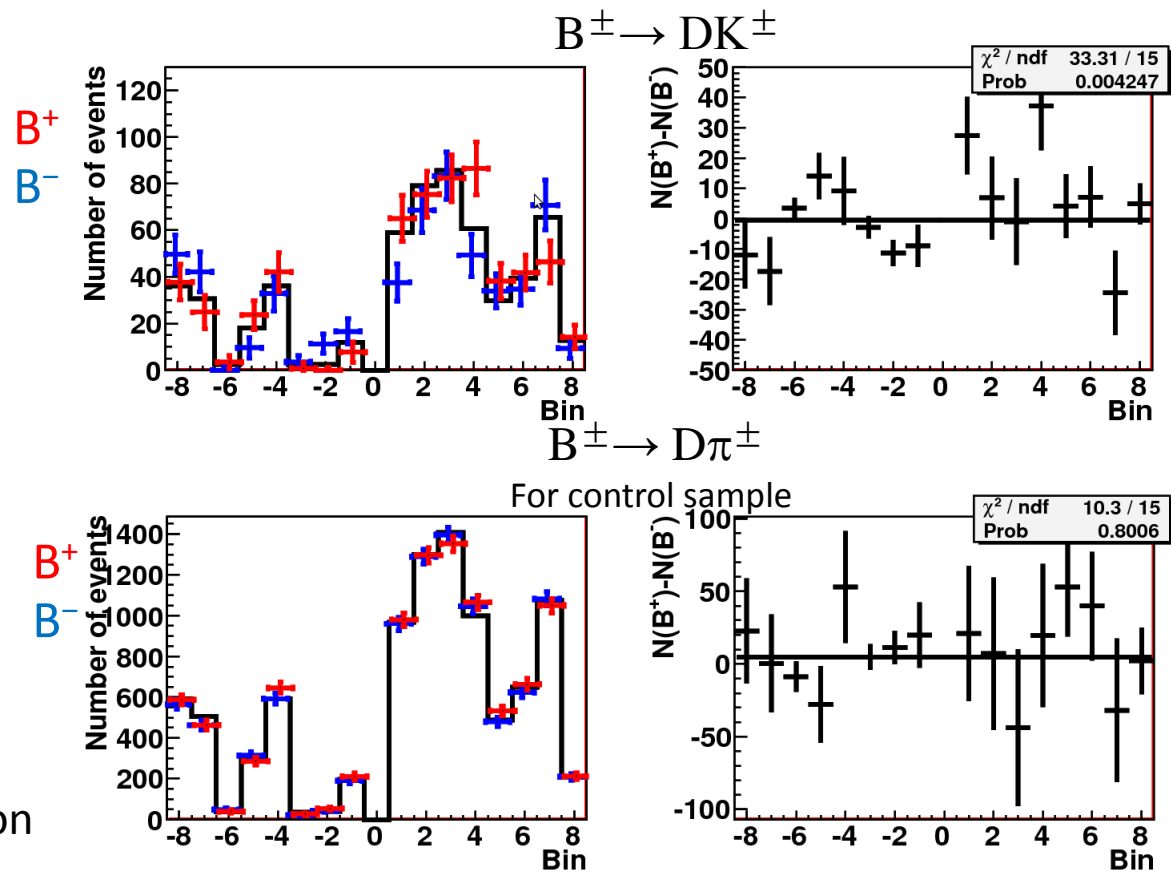
new
772M
Belle Preliminary

$$B^\mp \rightarrow D^0 K^\mp, D^0 \rightarrow K_S \pi\pi$$

$\cos\theta_{thr} < 0.8, |\Delta E| < 0.03 \text{ GeV}$



- Using reprocessed data.
 - Signal selection optimization
- Eff. increased $\sim 55\%$



$$M_i^\pm = h \{ K_i + r_B^2 K_{-i} + 2\sqrt{K_i K_{-i}} (x_\pm c_i + y_\pm s_i) \}$$

where $\left\{ \begin{array}{l} M_i^\pm: \text{numbers of events in } D \rightarrow K_S^0 \pi^+ \pi^- \text{ bins from } B^\pm \rightarrow DK^\pm \\ x_\pm = r_B \cos(\delta_B \pm \phi_3) \quad y_\pm = r_B \sin(\delta_B \pm \phi_3) \\ c_i = \langle \cos \Delta \delta_D \rangle, s_i = \langle \sin \Delta \delta_D \rangle \\ K_i: \text{numbers of events in bins of flavor } \bar{D}^0 \rightarrow K_S^0 \pi^+ \pi^- \text{ from } D^* \rightarrow D\pi. \end{array} \right.$

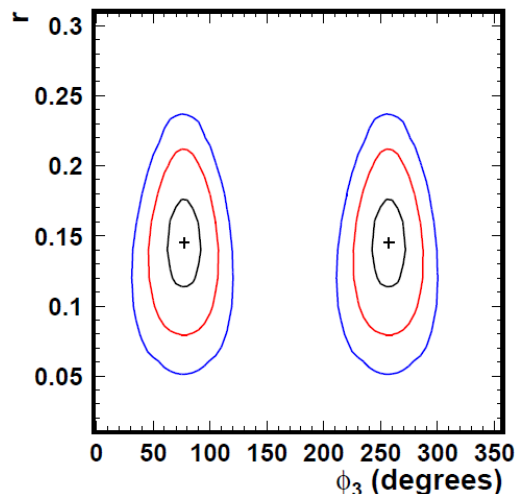
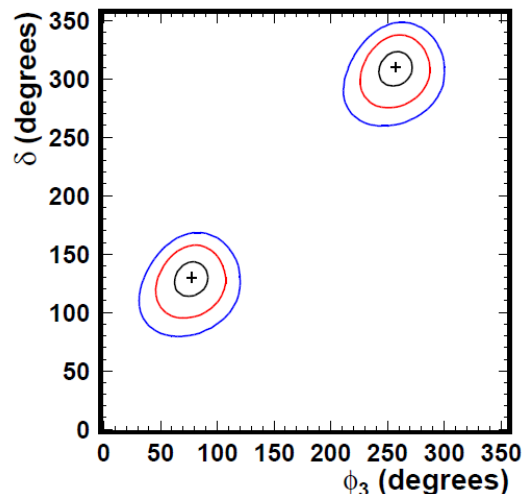
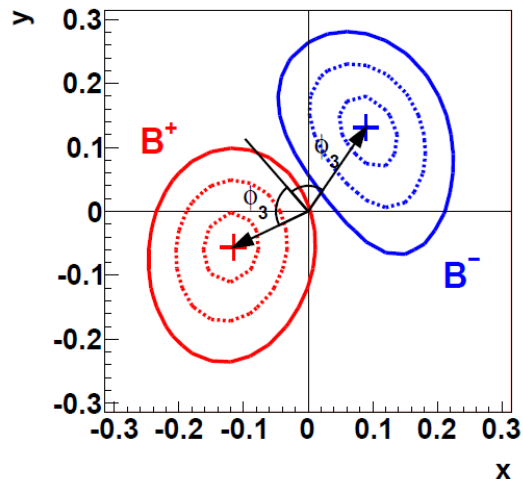
Dalitz analysis results of $B^- \rightarrow D^{(*)} K^{(*)-}, D \rightarrow K_S h^+ h^-$

new



772M

Belle Preliminary



$$x_- = +0.095 \pm 0.045 \pm 0.014 \pm 0.017$$

$$y_- = +0.137 \begin{array}{l} +0.053 \\ -0.057 \end{array} \pm 0.019 \pm 0.029$$

$$x_+ = -0.110 \pm 0.043 \pm 0.014 \pm 0.016$$

$$y_+ = -0.050 \begin{array}{l} +0.052 \\ -0.055 \end{array} \pm 0.011 \pm 0.021$$

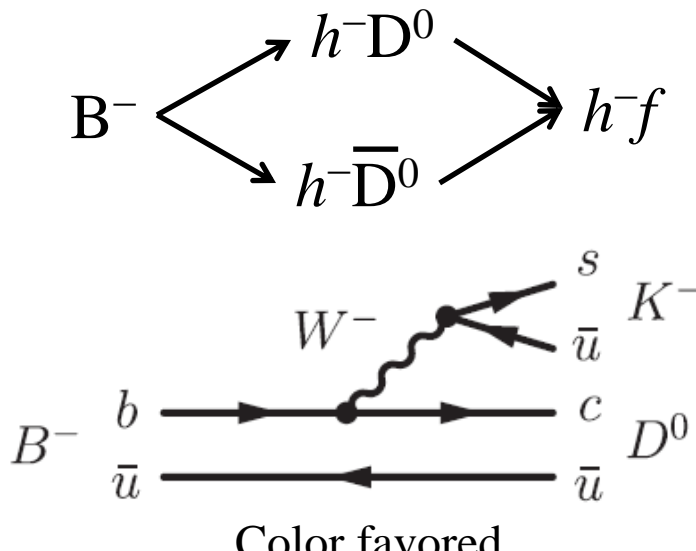
$$\phi_3 = (77.3_{-14.9}^{+15.1} \pm 4.2 \pm 4.3(c_i, s_i))^\circ$$

$$r_B = 0.145 \pm 0.030 \pm 0.011 \pm 0.011$$

$$\delta_B = (129.9 \pm 15.0 \pm 3.9 \pm 4.7)^\circ$$

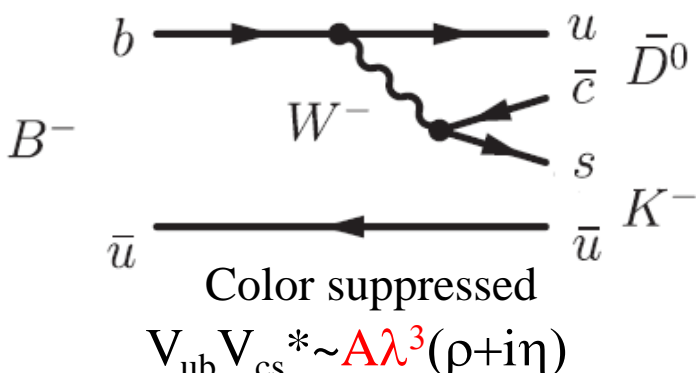
ADS Analyses of $B^- \rightarrow D^{(*)} K^{(*)-}$

D. Atwood, I. Dunietz, and A. Soni, PRL. 78,3257 (1997); PRD 63, 036005 (2001).



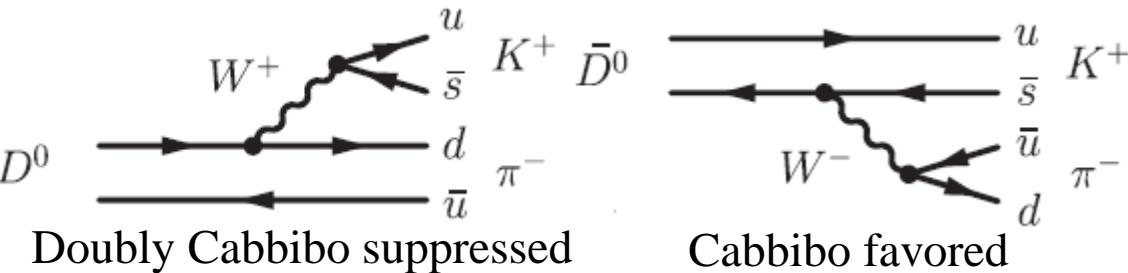
Color favored

$$V_{cb} V_{us} * \sim A \lambda^3$$



$$V_{ub} V_{cs} * \sim A \lambda^3 (\rho + i\eta)$$

where $f = K^+ \pi^-, K^+ \pi^- \pi^0, K^+ \pi^- \pi^+ \pi^-, \dots$



Doubly Cabibbo suppressed

Cabibbo favored

Choosing both contributing decay amplitudes are of comparable size.

$$R_{ADS} \equiv \frac{B(B^- \rightarrow D_{sup} h^-)}{B(B^- \rightarrow D_{fav} h^-)} = r_B^2 + r_D^2 + 2r_B r_D \cos\delta \cos\phi_3$$

$$\text{where } r_B \equiv \frac{A(B^- \rightarrow \bar{D}^0 K^-)}{A(B^- \rightarrow D^0 K^-)}$$

$$r_D \equiv \frac{A(D^0 \rightarrow K^+ \pi^-)}{A(D^0 \rightarrow K^- \pi^+)} = 0.0578 \pm 0.0008$$

$\delta_{B,D}$: Strong phase difference

ADS measurements at Belle

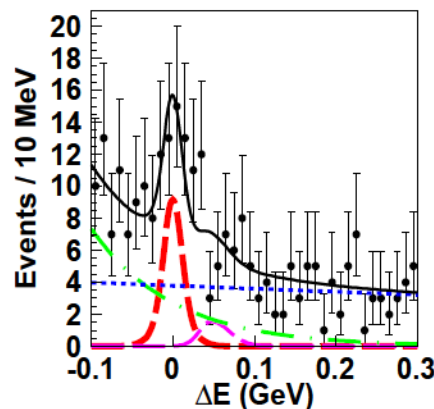


772M
new

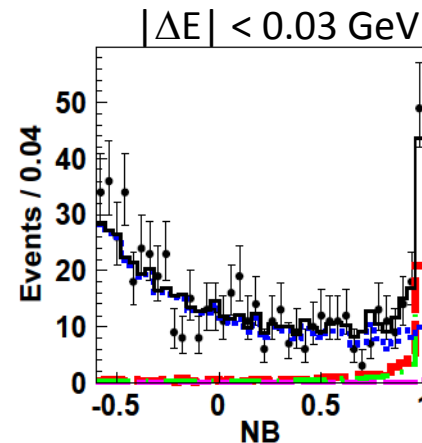
Y.Horii et al.,
arXiv:1103.5951v1
to appear in PRL
 $B^- \rightarrow DK^-$, $D \rightarrow K^-\pi^+$
(favored mode)

Suppressed mode $D \rightarrow K^+\pi^-$

$NB > 0.9$



$|\Delta E| < 0.03 \text{ GeV}$



NB: neural-network output for discriminating continuum background.

$$\mathcal{R}_{DK} = [1.63^{+0.44+0.07}_{-0.41-0.13}] \times 10^{-2},$$

$$\mathcal{R}_{D\pi} = [3.28^{+0.38+0.12}_{-0.36-0.18}] \times 10^{-3},$$

$$\mathcal{A}_{DK} = -0.39^{+0.26+0.04}_{-0.28-0.03}$$

$$\mathcal{A}_{D\pi} = -0.04 \pm 0.11^{+0.02}_{-0.01}$$

Belle reports the first evidence for $B^+ \rightarrow DK^+$, $D^0 \rightarrow K^+\pi^-$ with a significance of 4.1σ

ADS measurements at BaBar



467M

new

P. del Amo Sanchez et al.,
PRD82,072006(2010)

$B^- \rightarrow D K^-$, $D \rightarrow K^- \pi^+$

(favored mode)

$B^- \rightarrow D^* K^-$,
 $D^* \rightarrow D \pi^0$

$D \rightarrow K^- \pi^+$

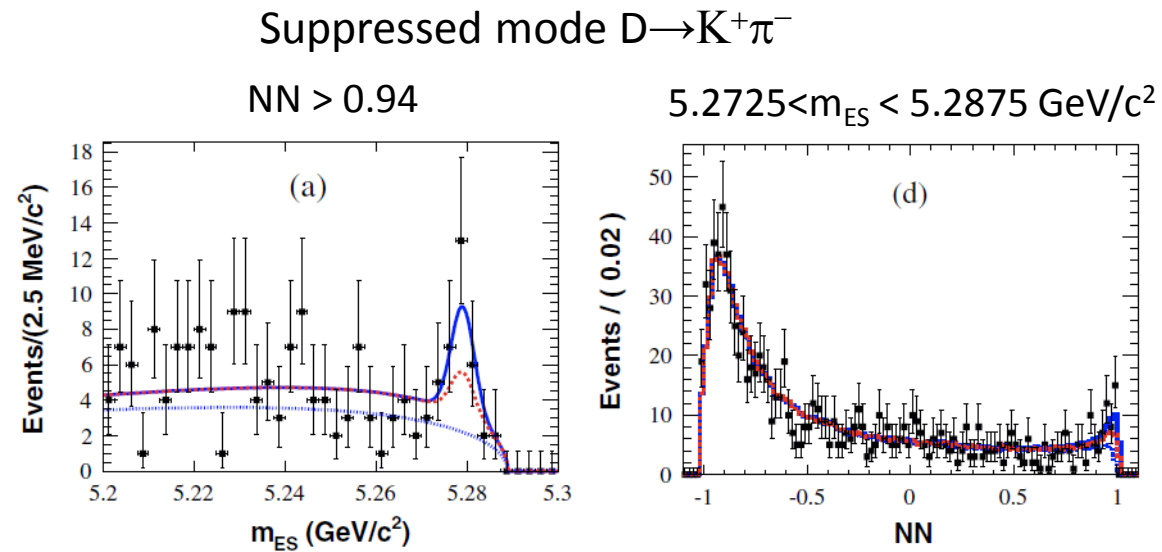
(favored mode)

$B^- \rightarrow D^* K^-$

$D^* \rightarrow D \gamma$

$D \rightarrow K^- \pi^+$

(favored mode)



$$\mathcal{R}_{DK} = (1.1 \pm 0.6 \pm 0.2) \times 10^{-2}.$$

$$\mathcal{R}_{(D\gamma)K}^* = (1.3 \pm 1.4 \pm 0.8) \times 10^{-2}.$$

$$\mathcal{R}_{(D\pi^0)K}^* = (1.8 \pm 0.9 \pm 0.4) \times 10^{-2}.$$

$$\mathcal{A}_{DK} = -0.86 \pm 0.47^{+0.12}_{-0.16}.$$

$$\mathcal{A}_{(D\pi^0)K}^* = +0.77 \pm 0.35 \pm 0.12.$$

$$\mathcal{A}_{(D\gamma)K}^* = +0.36 \pm 0.94^{+0.25}_{-0.41}.$$

BaBar reports $B^- \rightarrow D^{(*)} K^-$ followed by $D^* \rightarrow D\gamma, D\pi^0$ and $D \rightarrow K^- \pi^+$

ADS Results of $B^- \rightarrow D^{(*)} K^{(*)-}$ and $B^- \rightarrow D^{(*)} \pi^-$

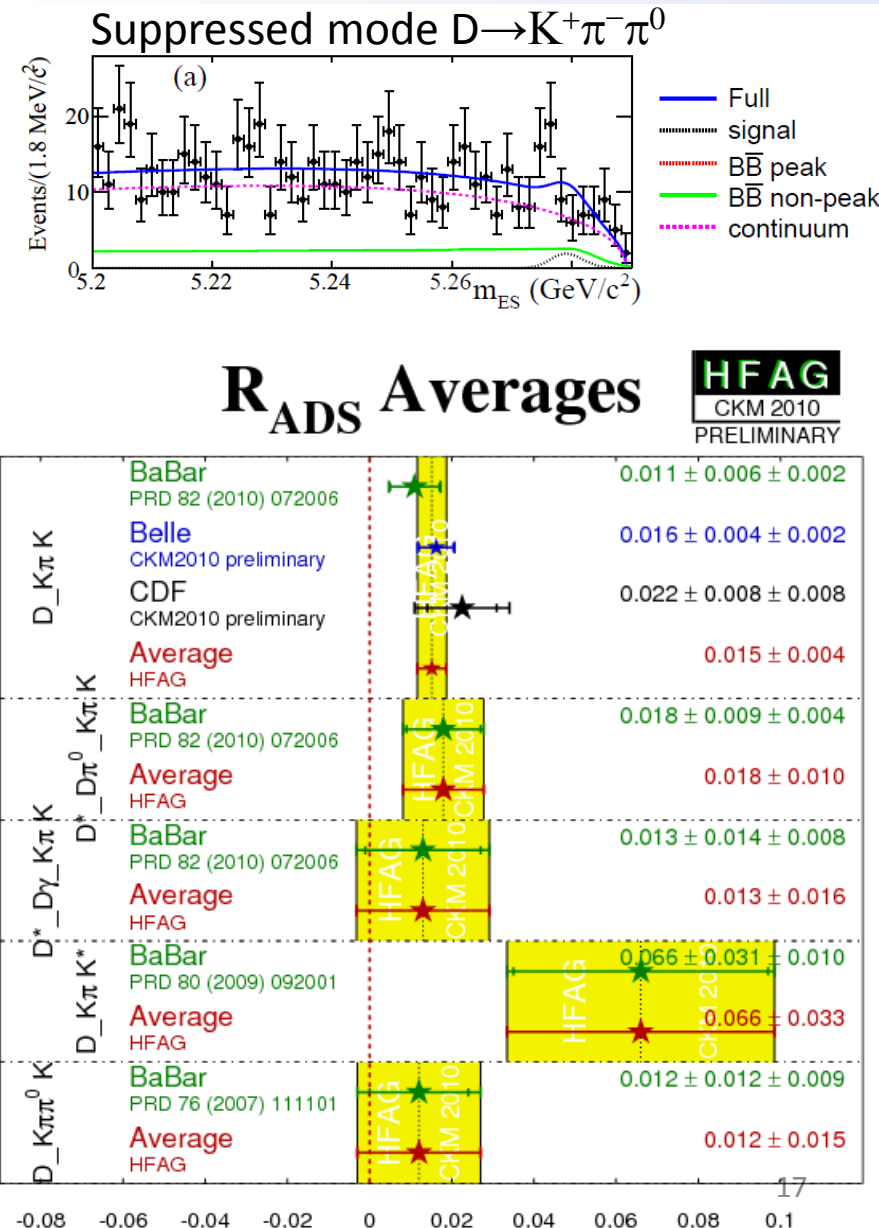
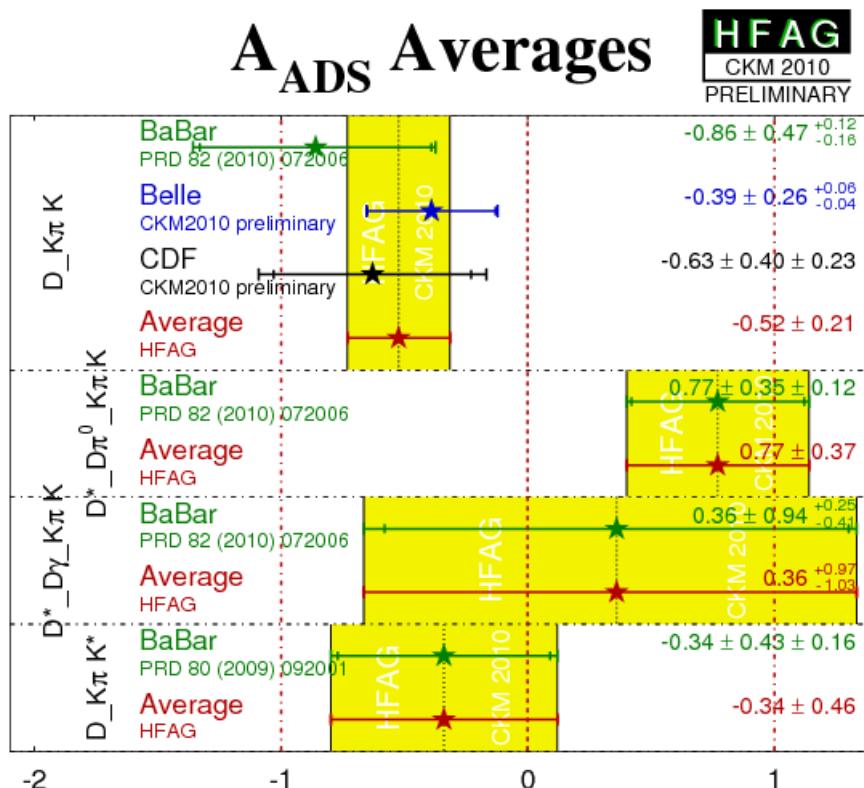


J. P. Lees et al., arXiv:1104.4472

R_{ADS} with $B^+ \rightarrow DK^+$, $D \rightarrow K^- \pi^+ \pi^0$
(favored mode)

$$R_{ADS} = (9.1^{+8.2}_{-7.6} {}^{+1.4}_{-3.7}) \times 10^{-3}$$

$R_{ADS} < 21 \times 10^{-3}$ at 90% probability.



GLW Analyses of $B^- \rightarrow D^{(*)}K^{(*)-}$

M. Gronau and D. London, Phys. Lett. B **253**, 483 (1991);
 M. Gronau and D. Wyler, Phys. Lett. B **265**, 172 (1991).

Defining the two CP eigenstates

$$|D_{CP\pm}^0\rangle = \frac{1}{\sqrt{2}} (|D^0\rangle \pm |\bar{D}^0\rangle)$$

where D_{CP+} :

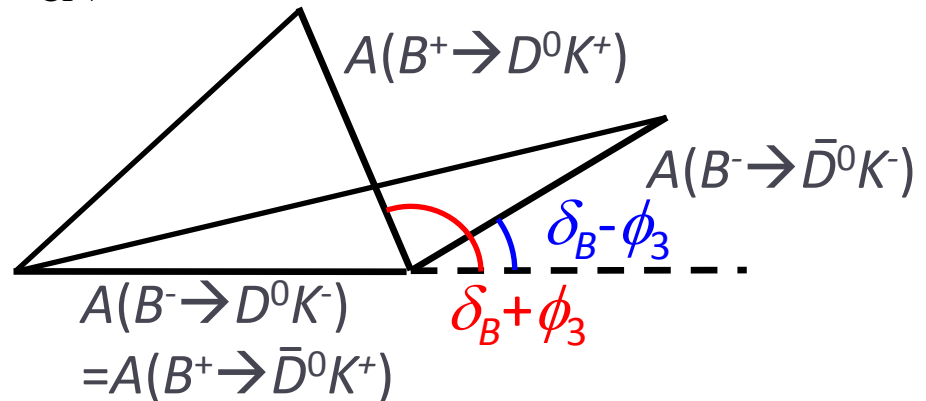
$KK, \pi\pi, \dots$ (CP even)

where D_{CP-} :

$K_S\pi^0, K_S\omega, K_S\phi, \dots$ (CP odd)

one can write $B \rightarrow D_{CP+}$ decays as

$$\begin{cases} \sqrt{2}A(B^+ \rightarrow D_{CP+}^0 K^+) = A(B^+ \rightarrow D^0 K^+) + A(B^+ \rightarrow \bar{D}^0 K^+) \\ \sqrt{2}A(B^- \rightarrow D_{CP+}^0 K^-) = A(B^- \rightarrow D^0 K^-) + A(B^- \rightarrow \bar{D}^0 K^-) \end{cases}$$



Observable

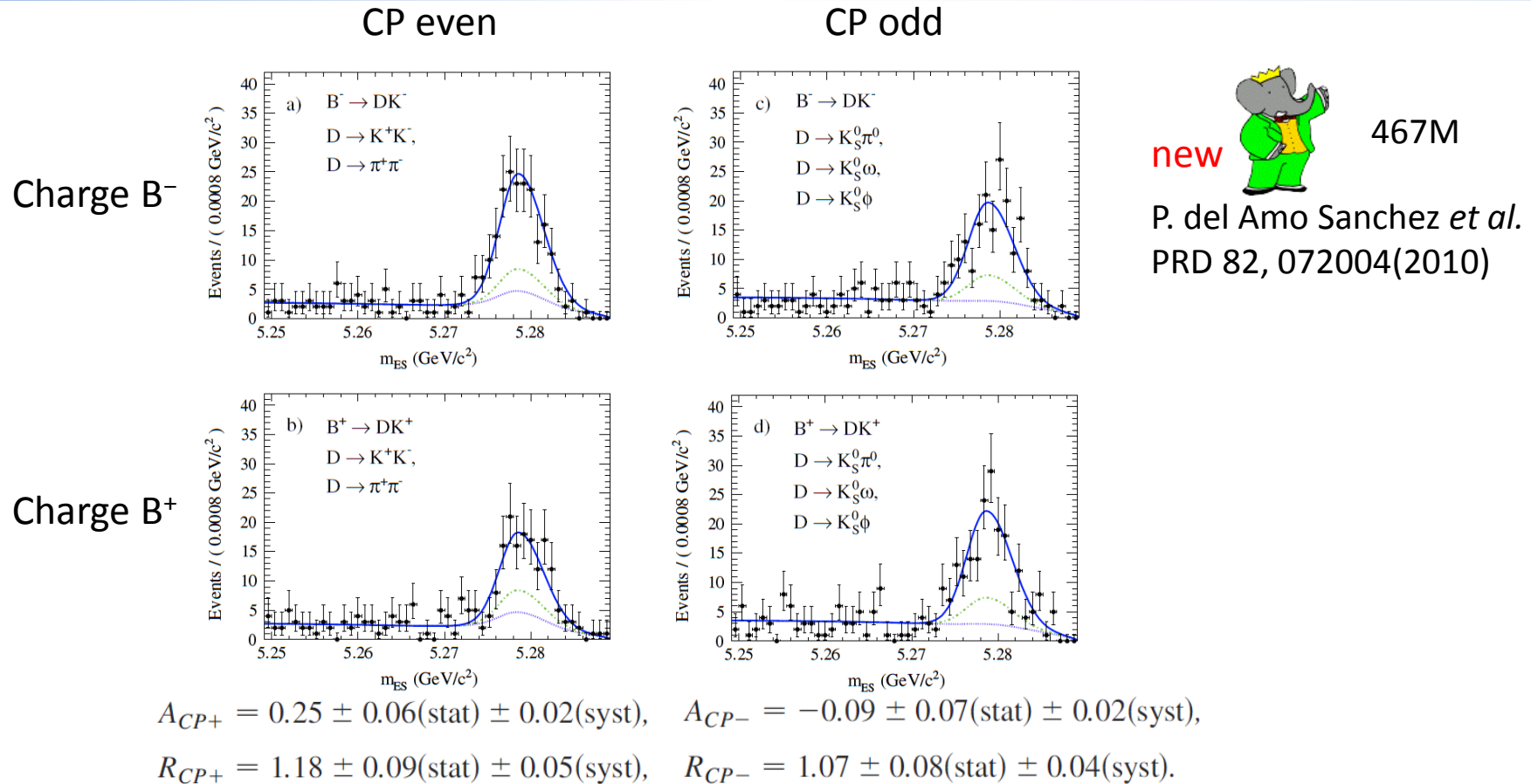
$$A_{CP\pm} \equiv \frac{\mathcal{B}(B^- \rightarrow D_{CP\pm}^0 K^-) - \mathcal{B}(B^+ \rightarrow D_{CP\pm}^0 K^+)}{\mathcal{B}(B^- \rightarrow D_{CP\pm}^0 K^-) + \mathcal{B}(B^+ \rightarrow D_{CP\pm}^0 K^+)} = \frac{2r_B \sin\delta_B \sin\phi_3}{1+r_B^2+2r_B \cos\delta_B \cos\phi_3}$$

Observable

$$R_{CP\pm} \equiv \frac{\mathcal{B}(B^- \rightarrow D_{CP\pm}^0 K^-) + \mathcal{B}(B^+ \rightarrow D_{CP\pm}^0 K^+)}{\mathcal{B}(B^- \rightarrow D^0 K^-) + \mathcal{B}(B^+ \rightarrow \bar{D}^0 K^+)} = 1+r_B^2+2r_B \cos\delta_B \cos\phi_3$$

where $r_B \equiv \frac{A(B^- \rightarrow \bar{D}^0 K^-)}{A(B^- \rightarrow D^0 K^-)}$, δ_B : strong phase difference₁₈

GLW measurements



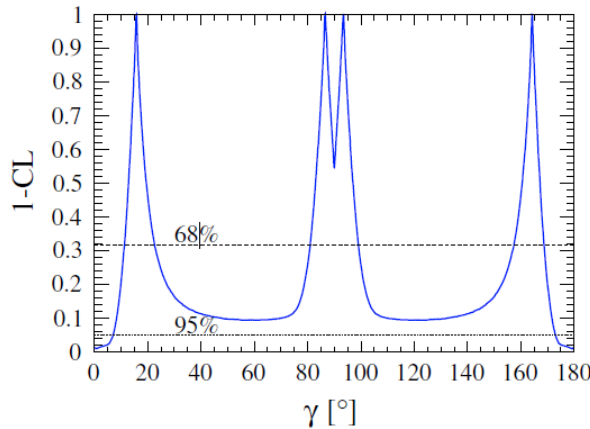
Direct CPV A_{CP+} 3.6σ away from 0

Translations to γ , r_B , δ_B

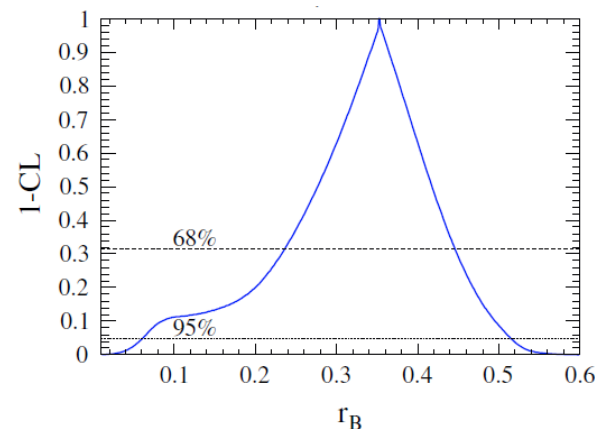
$$\mathcal{L}(\gamma, \delta_B, r_B) = \frac{1}{N} \exp\left(-\frac{1}{2}(\vec{y} - \vec{y}_t)^T V_{\text{cov}}^{-1}(\vec{y} - \vec{y}_t)\right)$$

$$\chi^2(\gamma, \delta_B, r_B) = -2 \ln \mathcal{L}(\gamma, \delta_B, r_B).$$

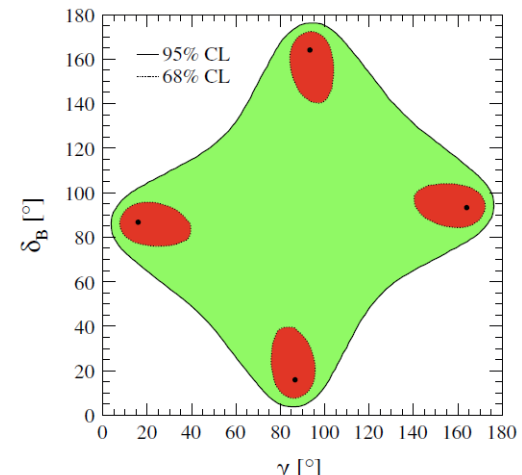
frequentist approach



68% CL [11.3, 22.7], [80.8, 99.2], [157.3, 168.7]



[0.24, 0.45]



[353.0, 360]

Also, exclude $D \rightarrow K_S \phi$, $\phi \rightarrow K^+ K^-$ events and applied event selection $K h^+ h^-$

$$x_{\pm} = r_B \cos(\delta_B \pm \gamma) \quad \left\{ \begin{array}{l} A_{CP-} = -0.08 \pm 0.07(\text{stat}) \pm 0.02(\text{syst}), \\ R_{CP-} = 1.03 \pm 0.09(\text{stat}) \pm 0.04(\text{syst}). \end{array} \right.$$

$$\quad \left\{ \begin{array}{l} x_+ = -0.057 \pm 0.039(\text{stat}) \pm 0.015(\text{syst}), \\ x_- = 0.132 \pm 0.042(\text{stat}) \pm 0.018(\text{syst}), \end{array} \right.$$

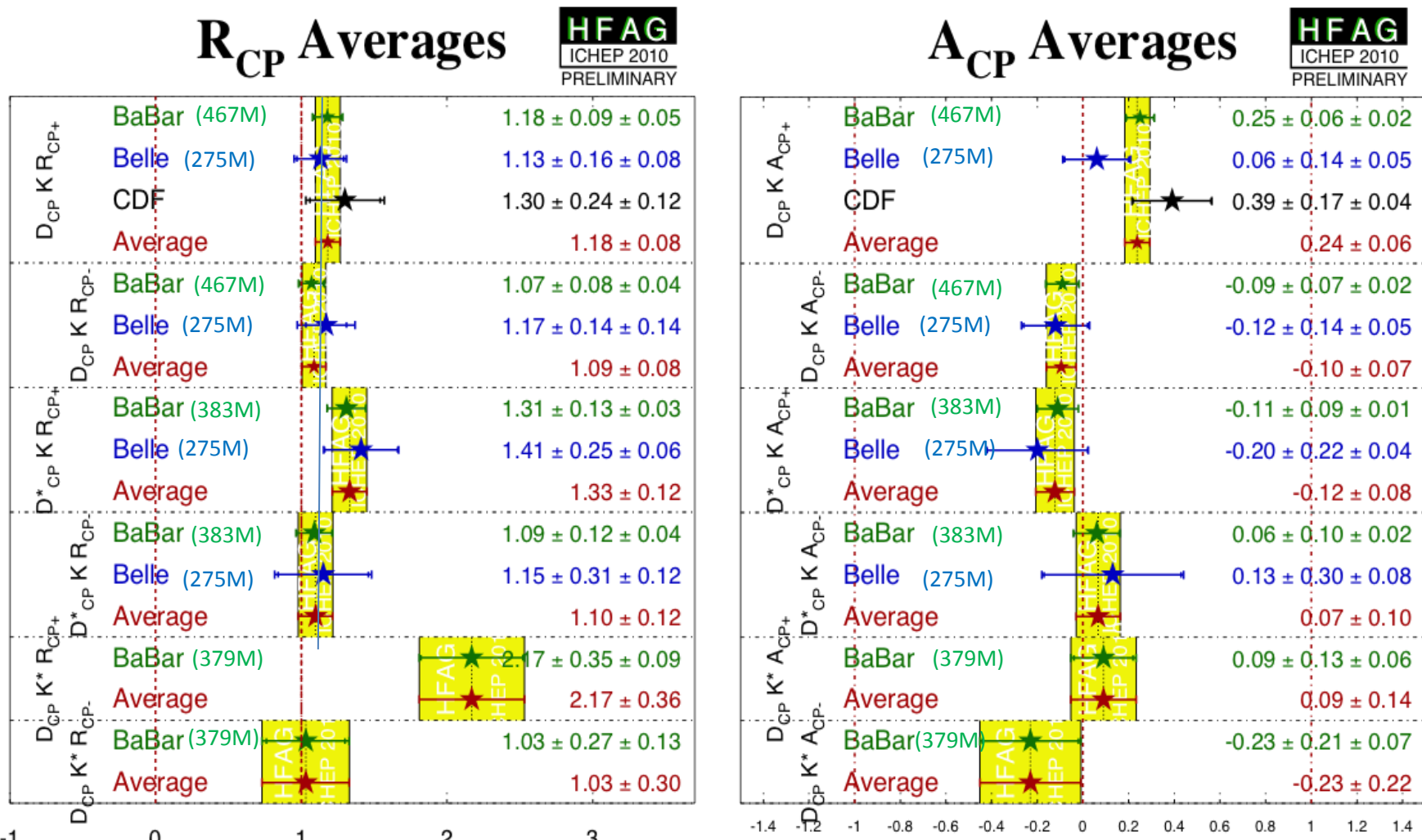
Agreement with the current Dalitz analysis.

new
467M



P. del Amo Sanchez *et al.*
PRD 82, 072004(2010)

GLW Results of $B^- \rightarrow D^*(*)K^*(-)$



Currently, BaBar measurements are dominant in precision.

With the full data sample and improved tracking,
final Belle measurements will have comparable or better errors.

Summary

- Model-dependent unbinned Dalitz plot analysis of $B \rightarrow D^{(*)} K$, $D \rightarrow K_S \pi \pi$ in Belle.
 $\phi_3 = (78.4^{+10.8}_{-11.6} \pm 3.6 \pm 8.9(\text{model}))^\circ$ A.Poluektov *et al.*, PRD 81, 112002(2010)
- Model-dependent unbinned Dalitz plot analysis of $B \rightarrow D^{(*)} K^{(*)}$, $D \rightarrow K_S \pi \pi$ and $K_S K K$ in BaBar.
 $\phi_3 = (68 \pm 14 \pm 4 \pm 3(\text{model}))^\circ$ P. del Amo Sanchez *et al.*, PRL 105, 121801(2010)
- First model-independent unbinned Dalitz plot analysis of $B \rightarrow D K$, $D \rightarrow K_S \pi \pi$ in Belle.
 $\phi_3 = (77.3^{+15.1}_{-14.9} \pm 4.2 \pm 4.3(c_i, s_i))^\circ$ Belle Preliminary
- First evidence of ADS R_{DK} with $B^- \rightarrow D K^-$, $D \rightarrow K^- \pi^+$ at 4.1σ in Belle. $\mathcal{R}_{DK} = [1.63^{+0.44}_{-0.41}({}^{+0.07}_{-0.13}(\text{syst}))] \times 10^{-2}$, Y.Horii *et al.*, arXiv:1103.5951v1 accepted to PRL
- Direct CPV GLW A_{CP+} in $B \rightarrow D K$, $D \rightarrow K K$ and $\pi \pi$ at 3.6σ in BaBar. $A_{CP+} = 0.25 \pm 0.06(\text{stat}) \pm 0.02(\text{syst})$, P. del Amo Sanchez *et al.*, PRD 82, 072004(2010)
- New ϕ_3/γ results from e^+e^- colliders are coming soon.

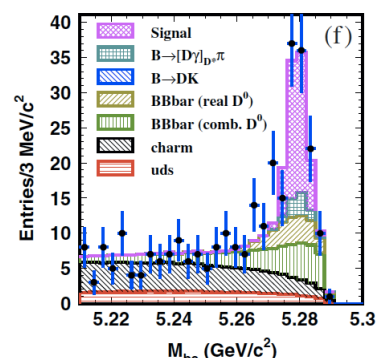
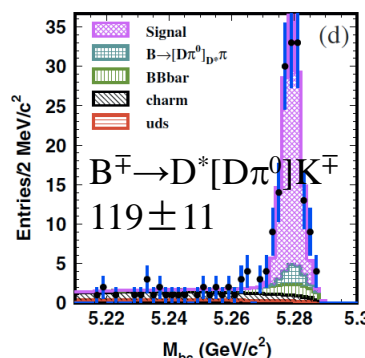
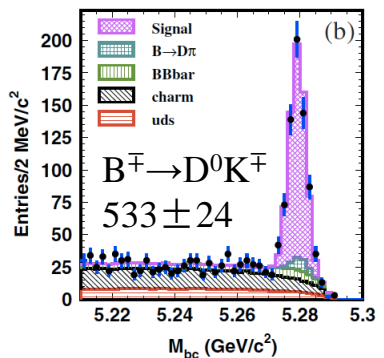
Backup slides

Yields of $B^- \rightarrow D^{(*)} K^{(*)-}$ with $D \rightarrow K_S h^+ h^-$

657M



A. Poluektov *et al.*,
PRD 81, 112002 (2010)

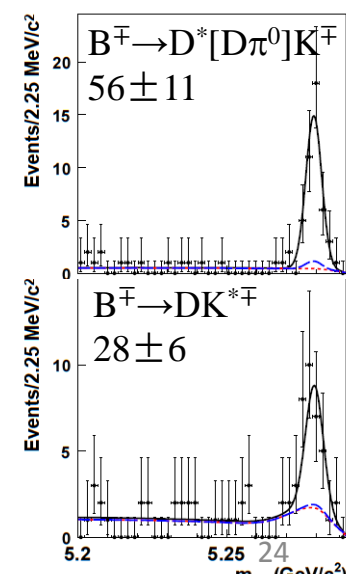
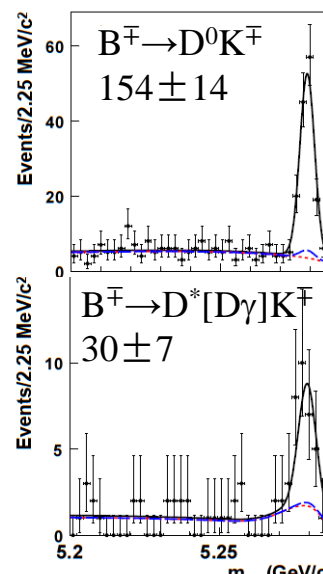
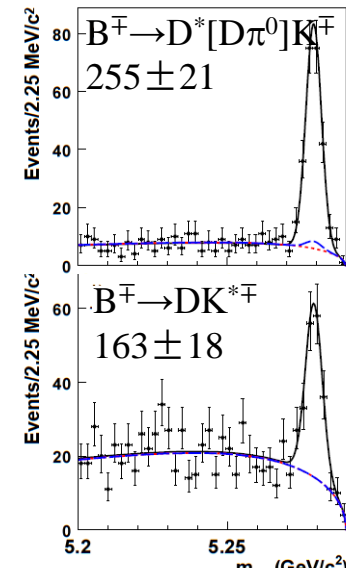
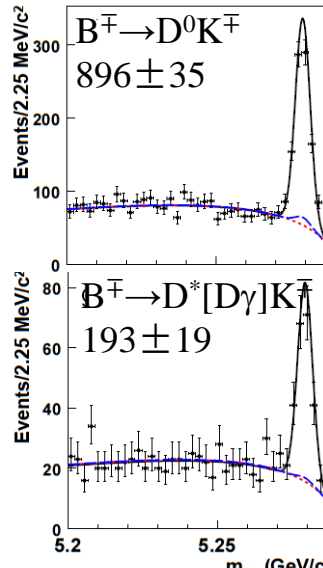


468M



P. del Amo Sanchez *et al.*,
PRL 105, 121801 (2010)

1507 $D^0 \rightarrow K_S \pi\pi$



268 $D^0 \rightarrow K_S KK$

Previous results of Dalitz plot analysis

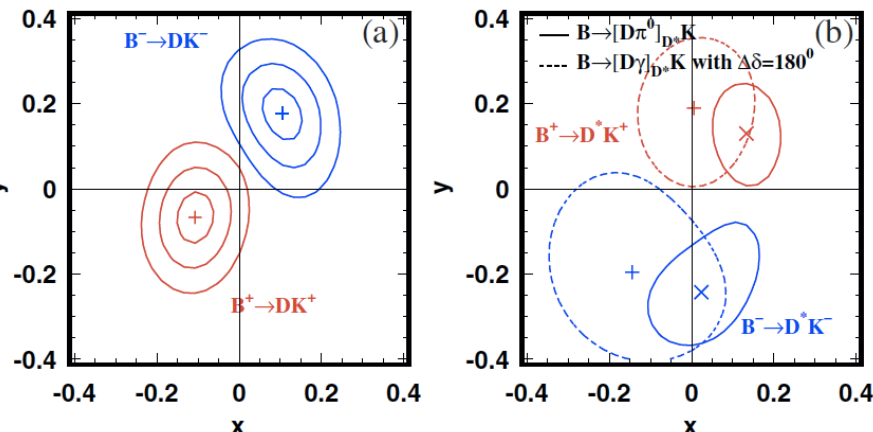


A. Poluektov *et al.*,

PRD 81, 112002 (2010)

$B^\pm \rightarrow D^{(*)} K^\pm, D \rightarrow K_S \pi^+ \pi^-$

657M



$$\phi_3 = (76^{+12}_{-13} \pm 4 \pm 9(\text{model}))^\circ$$

$$r_{DK} = 0.160^{+0.040}_{-0.038} \pm 0.011^{+0.050}_{-0.010}$$

$$r_{D^*K} = 0.196^{+0.072}_{-0.069} \pm 0.012^{+0.062}_{-0.012}$$

$$\delta_{DK} = (136.7^{+13.0}_{-15.8} \pm 4.0 \pm 22.9)^\circ$$

$$\delta_{D^*K} = (341.9^{+18.0}_{-19.6} \pm 3.0 \pm 22.9)^\circ$$

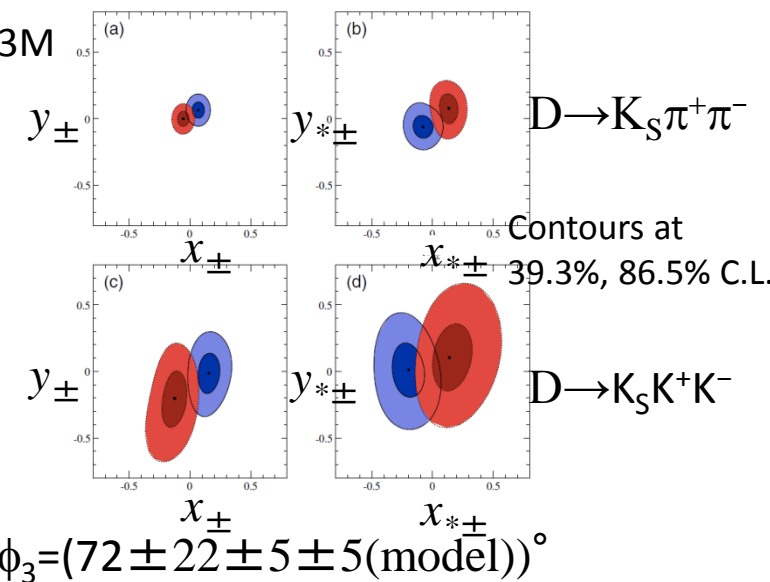


AUBERT *et al.*,

PRD 78, 054023 (2008)

$B^\pm \rightarrow D^{(*)} K^\pm, D \rightarrow K_S \pi^+ \pi^-, K_S K^+ K^-$

383M



$$\phi_3 = (72 \pm 22 \pm 5 \pm 5(\text{model}))^\circ$$

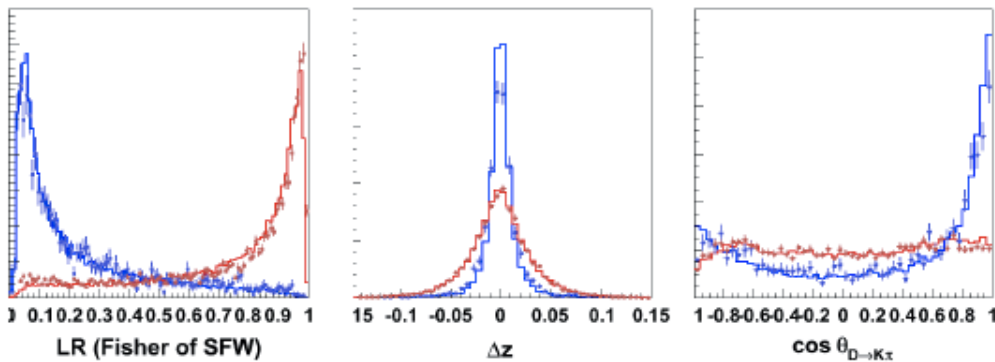
Both the measurements are adopted model-dependent Dalitz analysis.

Continuum Suppression

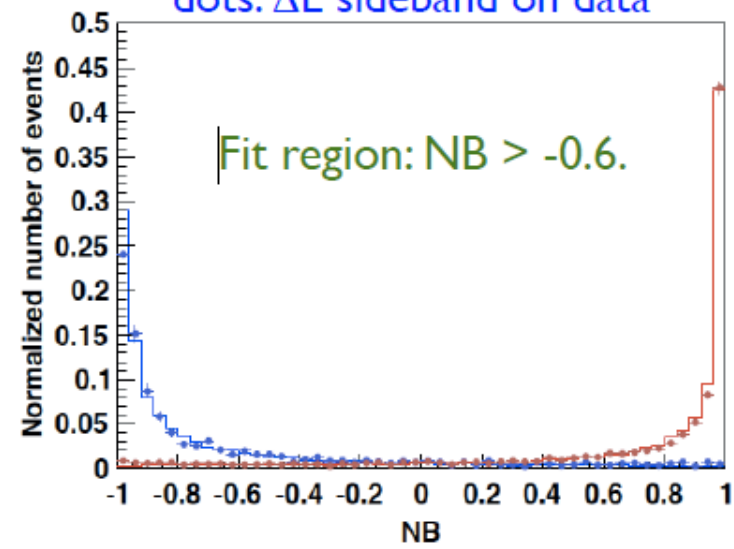
- ▶ Main background is $e^+e^- \rightarrow q\bar{q}$ ($q=u, d, s, c$) continuum process.
- ▶ To discriminate this background, new technique employs NeuroBayes (NB) neural network.

NB inputs (10 in total):

- LR for Fisher of SFW moments
- Vertex separation between reconstructed B and the other B (Δz)
- Decay angle for $D \rightarrow K\pi$
- ...



histogram: signal on MC
dots: Calib. mode ($D\pi$) on data
histogram: $q\bar{q}$ on MC
dots: ΔE sideband on data



Belle model-dep. DP syst.

| Source of uncertainty | Δx_- | Δy_- | Δx_+ | Δy_+ |
|--|--------------|--------------|--------------|--------------|
| Dalitz plot efficiency | ± 3.0 | ± 1.9 | ± 3.2 | ± 1.6 |
| Crossfeed between bins | $+0.4$ | $+3.0$ | -0.7 | -0.9 |
| Signal shape | | | | |
| Parametrization | | | | |
| $(M_{bc}, \Delta E)$ | -0.2 | +0.5 | +0.2 | -4.8 |
| $(\cos \theta_{thr}, \mathcal{F})$ | -0.5 | -1.5 | -0.8 | -1.3 |
| Correlation btw. $(M_{bc}, \Delta E)$ and $(\cos \theta_{thr}, \mathcal{F})$ | +0.2 | +0.5 | +0.0 | -0.2 |
| MC uncertainty in $(\cos \theta_{thr}, \mathcal{F})$ | -0.5 | -1.0 | -0.5 | -0.7 |
| Correlation with Dalitz plot | +0.5 | -0.1 | -0.6 | +0.1 |
| u, d, s, c continuum shape | | | | |
| Off-resonance data uncertainty in $(M_{bc}, \Delta E)$ | -0.2 | +0.2 | -0.1 | -0.2 |
| Parametrization | | | | |
| $(M_{bc}, \Delta E)$ | +0.3 | +0.7 | +0.2 | -0.6 |
| $(\cos \theta_{thr}, \mathcal{F})$ | +0.2 | +1.1 | -0.1 | +0.5 |
| Correlation btw. $(M_{bc}, \Delta E)$ and $(\cos \theta_{thr}, \mathcal{F})$ | +0.8 | +0.6 | +0.8 | +1.0 |
| Random $B\bar{B}$ shape | | | | |
| Parametrization | | | | |
| $(M_{bc}, \Delta E)$ | +0.2 | +0.3 | +0.2 | +0.2 |
| $(\cos \theta_{thr}, \mathcal{F})$ | +0.3 | +0.7 | +0.4 | +0.3 |
| Correlation btw. $(M_{bc}, \Delta E)$ and $(\cos \theta_{thr}, \mathcal{F})$ | -0.2 | -0.6 | -0.2 | -0.3 |
| Dalitz distribution | +3.2 | -0.7 | +4.5 | -0.6 |
| MC uncertainty | | | | |
| $(M_{bc}, \Delta E)$ | -0.5 | -1.1 | -0.4 | -0.7 |
| $(\cos \theta_{thr}, \mathcal{F})$ | +0.0 | +0.1 | -0.1 | +0.3 |
| Peaking $B\bar{B}$ shape | | | | |
| Parametrization | < 0.1 | < 0.1 | < 0.1 | < 0.1 |
| MC uncertainty | < 0.1 | < 0.1 | < 0.1 | < 0.1 |
| c_i, s_i precision | ± 2.6 | ± 6.5 | ± 2.6 | ± 6.5 |
| Flavor-tagged statistics | ± 1.7 | ± 2.0 | ± 1.6 | ± 2.0 |
| Fit bias | ± 0.4 | ± 0.5 | ± 0.4 | ± 0.5 |
| Total without c_i, s_i precision | ± 5.0 | ± 5.0 | ± 6.0 | ± 6.0 |
| Total | ± 5.6 | ± 8.2 | ± 6.5 | ± 8.8 |

BaBar model-dep. Prev. DP syst.

TABLE V. Summary of the main contributions to the Dalitz model systematic error on the CP parameters.

| Source | x_- | y_- | x_+ | y_+ | x_-^* | y_-^* | x_+^* | y_+^* | x_{s-} | y_{s-} | x_{s+} | y_{s+} |
|---------------------------------------|-------|-------|-------|-------|---------|---------|---------|---------|----------|----------|----------|----------|
| Mass and width of Breit-Wigner's | 0.001 | 0.001 | 0.001 | 0.002 | 0.001 | 0.002 | 0.001 | 0.003 | 0.003 | 0.001 | 0.002 | 0.002 |
| $\pi\pi$ S-wave K -matrix solutions | 0.003 | 0.012 | 0.003 | 0.001 | 0.003 | 0.007 | 0.002 | 0.009 | 0.001 | 0.001 | 0.013 | 0.003 |
| $K\pi$ S-wave parametrization | 0.001 | 0.001 | 0.002 | 0.004 | 0.001 | 0.003 | 0.001 | 0.003 | 0.005 | 0.001 | 0.004 | 0.002 |
| Angular dependence | 0.001 | 0.001 | 0.001 | 0.001 | 0.001 | 0.001 | 0.002 | 0.001 | 0.003 | 0.001 | 0.003 | 0.001 |
| Blatt-Weisskopf radius | 0.001 | 0.001 | 0.001 | 0.001 | 0.001 | 0.001 | 0.001 | 0.001 | 0.002 | 0.001 | 0.001 | 0.003 |
| Add/remove resonances | 0.001 | 0.001 | 0.001 | 0.001 | 0.001 | 0.002 | 0.001 | 0.002 | 0.001 | 0.001 | 0.001 | 0.002 |
| Dalitz plot efficiency | 0.006 | 0.004 | 0.008 | 0.001 | 0.002 | 0.004 | 0.002 | 0.003 | 0.008 | 0.001 | 0.008 | 0.004 |
| Background Dalitz plot shape | 0.003 | 0.002 | 0.004 | 0.001 | 0.001 | 0.001 | 0.001 | 0.001 | 0.004 | 0.001 | 0.004 | 0.002 |
| Normalization and binning | 0.001 | 0.001 | 0.001 | 0.002 | 0.001 | 0.001 | 0.001 | 0.002 | 0.002 | 0.001 | 0.003 | 0.001 |
| Mistag rate | 0.008 | 0.006 | 0.006 | 0.005 | 0.002 | 0.001 | 0.002 | 0.003 | 0.008 | 0.010 | 0.004 | 0.007 |
| Dalitz plot complex amplitudes | 0.002 | 0.002 | 0.003 | 0.004 | 0.001 | 0.001 | 0.002 | 0.006 | 0.003 | 0.003 | 0.004 | 0.002 |
| Total Dalitz model | 0.011 | 0.015 | 0.011 | 0.008 | 0.004 | 0.010 | 0.005 | 0.012 | 0.014 | 0.011 | 0.018 | 0.010 |

Belle ADS syst.

| Source | R_{DK} | $R_{D\pi}$ | \mathcal{A}_{DK} | $\mathcal{A}_{D\pi}$ |
|---------------------|-----------------|--------------------|--------------------|----------------------|
| Fit | $\pm 26\%$ | $\pm 3.1\%$ | ± 0.40 | ± 0.04 |
| Peaking backgrounds | $^{+2}_{-25}\%$ | $^{+2.2}_{-5.3}\%$ | ... | ... |
| Efficiency | $\pm 2.7\%$ | $\pm 2.5\%$ | ... | ... |
| Detector asymmetry | ... | ... | ± 0.01 | ± 0.01 |

BaBar ADS syst.

TABLE V. Summary of systematic uncertainties on \mathcal{R} for $D^{(*)}\pi$, in units of 10^{-3} .

| Source | $\Delta\mathcal{R}(10^{-3})$ $D\pi$ | $\Delta\mathcal{R}(10^{-3})$ $D_{D\pi^0}^*\pi$ | $\Delta\mathcal{R}(10^{-3})$ $D_{D\gamma}^*\pi$ |
|--|--|---|--|
| Signal NN | ± 0.1 | ± 0.1 | ± 0.1 |
| $B\bar{B}$ background NN | ± 0.1 | ± 0.1 | ± 0.9 |
| $udsc$ background NN | ± 0.1 | ± 0.1 | ± 0.3 |
| $B\bar{B}$ combinatorial background shape (m_{ES}) | ± 0.2 | ± 0.1 | ± 0.2 |
| Peaking background WS | ± 0.2 | ± 0.8 | ± 2.0 |
| Peaking background RS | ± 0.0 | ± 0.1 | ± 0.1 |
| $B\bar{B}$ combinatorial background | - | ± 0.0 | ± 0.4 |
| Combined | ± 0.4 | ± 0.8 | ± 2.2 |

Belle model-indep. DP syst.

ϕ_3 : Systematic errors

Systematic errors in units 10^{-3} .

| Source of uncertainty | Δx_- | Δy_- | Δx_+ | Δy_+ |
|---|--------------|--------------|--------------|--------------|
| Dalitz plot efficiency | 4.8 | 2.0 | 5.6 | 2.1 |
| Crossfeed between bins | 0.4 | 9.0 | 0.6 | 3.0 |
| Signal shape | 7.3 | 7.4 | 7.3 | 5.1 |
| u, d, s, c continuum background | 6.7 | 5.6 | 6.6 | 3.2 |
| $B\bar{B}$ background | 7.8 | 12.2 | 7.2 | 6.1 |
| $B^\pm \rightarrow D\pi^\pm$ background | 1.2 | 4.2 | 1.9 | 1.9 |
| Flavor-tagged statistics | 1.5 | 2.7 | 1.7 | 1.9 |
| Fit bias | 3.2 | 5.8 | 3.2 | 5.8 |
| c_i, s_i precision | 10.1 | 22.5 | 7.2 | 17.4 |
| Total without c_i, s_i precision | ± 14.0 | ± 19.4 | ± 14.0 | ± 11.3 |
| Total | ± 17.3 | ± 29.7 | ± 15.7 | ± 20.7 |

CLEO ci,si result

TABLE IX. Fit results for c_i and s_i . The first error is statistical, the second error is the systematic uncertainty (excluding Δc_i , Δs_i), and the third error is the systematic uncertainty due to Δc_i and Δs_i that relate the $K_S^0\pi^+\pi^-$ and $K_L^0\pi^+\pi^-$ Dalitz-plot models.

| i | c_i | s_i |
|-----|--|--|
| 1 | $0.743 \pm 0.037 \pm 0.022 \pm 0.013$ | $0.014 \pm 0.160 \pm 0.077 \pm 0.045$ |
| 2 | $0.611 \pm 0.071 \pm 0.037 \pm 0.009$ | $0.014 \pm 0.215 \pm 0.055 \pm 0.017$ |
| 3 | $0.059 \pm 0.063 \pm 0.031 \pm 0.057$ | $0.609 \pm 0.190 \pm 0.076 \pm 0.037$ |
| 4 | $-0.495 \pm 0.101 \pm 0.052 \pm 0.045$ | $0.151 \pm 0.217 \pm 0.069 \pm 0.048$ |
| 5 | $-0.911 \pm 0.049 \pm 0.032 \pm 0.021$ | $-0.050 \pm 0.183 \pm 0.045 \pm 0.036$ |
| 6 | $-0.736 \pm 0.066 \pm 0.030 \pm 0.018$ | $-0.340 \pm 0.187 \pm 0.052 \pm 0.047$ |
| 7 | $0.157 \pm 0.074 \pm 0.042 \pm 0.051$ | $-0.827 \pm 0.185 \pm 0.060 \pm 0.036$ |
| 8 | $0.403 \pm 0.046 \pm 0.021 \pm 0.002$ | $-0.409 \pm 0.158 \pm 0.050 \pm 0.002$ |

TABLE X. Fit results for c'_i and s'_i . The first error is statistical, the second error is the systematic uncertainty (excluding Δc_i , Δs_i), and the third error is the systematic uncertainty due to Δc_i and Δs_i .

| i | c'_i | s'_i |
|-----|--|--|
| 1 | $0.840 \pm 0.037 \pm 0.023 \pm 0.014$ | $-0.021 \pm 0.160 \pm 0.080 \pm 0.036$ |
| 2 | $0.779 \pm 0.071 \pm 0.039 \pm 0.008$ | $-0.069 \pm 0.215 \pm 0.060 \pm 0.047$ |
| 3 | $0.250 \pm 0.063 \pm 0.029 \pm 0.102$ | $0.587 \pm 0.190 \pm 0.072 \pm 0.006$ |
| 4 | $-0.349 \pm 0.101 \pm 0.057 \pm 0.092$ | $0.275 \pm 0.217 \pm 0.067 \pm 0.058$ |
| 5 | $-0.793 \pm 0.049 \pm 0.029 \pm 0.036$ | $-0.016 \pm 0.183 \pm 0.046 \pm 0.042$ |
| 6 | $-0.546 \pm 0.066 \pm 0.028 \pm 0.038$ | $-0.388 \pm 0.187 \pm 0.056 \pm 0.072$ |
| 7 | $0.475 \pm 0.074 \pm 0.036 \pm 0.081$ | $-0.725 \pm 0.185 \pm 0.065 \pm 0.058$ |
| 8 | $0.591 \pm 0.046 \pm 0.021 \pm 0.011$ | $-0.374 \pm 0.158 \pm 0.059 \pm 0.054$ |

CLEO ci, si systematics

 TABLE V. Systematic uncertainties for c_i .

| | c_1 | c_2 | c_3 | c_4 | c_5 | c_6 | c_7 | c_8 |
|--------------------------------|-------|-------|-------|-------|-------|-------|-------|-------|
| $K_i^{(0)}$ statistics error | 0.010 | 0.015 | 0.016 | 0.019 | 0.009 | 0.015 | 0.018 | 0.008 |
| Momentum resolution | 0.008 | 0.015 | 0.012 | 0.019 | 0.011 | 0.012 | 0.017 | 0.009 |
| Efficiency variation | 0.004 | 0.007 | 0.011 | 0.008 | 0.005 | 0.008 | 0.010 | 0.006 |
| Single-tag yields | 0.006 | 0.007 | 0.013 | 0.011 | 0.005 | 0.008 | 0.015 | 0.008 |
| Tag side background | 0.007 | 0.007 | 0.014 | 0.013 | 0.006 | 0.008 | 0.014 | 0.011 |
| $K_S^0 \pi^+ \pi^-$ background | 0.001 | 0.002 | 0.009 | 0.027 | 0.012 | 0.006 | 0.003 | 0.002 |
| $K_L^0 \pi^+ \pi^-$ background | 0.006 | 0.018 | 0.004 | 0.024 | 0.017 | 0.012 | 0.020 | 0.006 |
| Multi-candidate selection | 0.002 | 0.003 | 0.003 | 0.008 | 0.004 | 0.006 | 0.003 | 0.002 |
| Non- D/\bar{D} | 0.010 | 0.016 | 0.004 | 0.007 | 0.004 | 0.005 | 0.006 | 0.005 |
| DCSD | 0.009 | 0.012 | 0.005 | 0.013 | 0.014 | 0.010 | 0.013 | 0.006 |
| Sum | 0.022 | 0.037 | 0.031 | 0.052 | 0.032 | 0.030 | 0.042 | 0.021 |

 TABLE VI. Systematic uncertainties for s_i .

| | s_1 | s_2 | s_3 | s_4 | s_5 | s_6 | s_7 | s_8 |
|--------------------------------|-------|-------|-------|-------|-------|-------|-------|-------|
| $K_i^{(0)}$ statistics error | 0.031 | 0.027 | 0.039 | 0.030 | 0.023 | 0.023 | 0.033 | 0.026 |
| Momentum resolution | 0.018 | 0.035 | 0.023 | 0.033 | 0.023 | 0.022 | 0.022 | 0.018 |
| Efficiency variation | 0.018 | 0.012 | 0.019 | 0.010 | 0.013 | 0.018 | 0.013 | 0.012 |
| Single-tag yields | 0.005 | 0.001 | 0.005 | 0.004 | 0.003 | 0.003 | 0.005 | 0.003 |
| Tag side background | 0.004 | 0.001 | 0.001 | 0.003 | 0.001 | 0.004 | 0.002 | 0.001 |
| $K_S^0 \pi^+ \pi^-$ background | 0.005 | 0.008 | 0.030 | 0.023 | 0.005 | 0.003 | 0.016 | 0.014 |
| $K_L^0 \pi^+ \pi^-$ background | 0.050 | 0.022 | 0.018 | 0.035 | 0.006 | 0.024 | 0.005 | 0.025 |
| Multi-candidate selection | 0.036 | 0.018 | 0.033 | 0.012 | 0.022 | 0.026 | 0.028 | 0.011 |
| Non- D/\bar{D} | 0.005 | 0.003 | 0.004 | 0.005 | 0.005 | 0.005 | 0.003 | 0.002 |
| DCSD | 0.023 | 0.004 | 0.030 | 0.019 | 0.015 | 0.006 | 0.027 | 0.020 |
| Sum | 0.077 | 0.055 | 0.076 | 0.069 | 0.045 | 0.052 | 0.060 | 0.050 |